J Electroceram (2009) 22:233–237
DOI 10.1007/s10832-007-9386-x

Crystal structure and the effect of annealing atmosphere on the dielectric properties of the spinels $MgAl_2O_4$, $NiFe_2O_4$, and $NiAlFeO_4$

Jeong Seog Kim · Kyoung Ho Lee · Chae Il Cheon

Received: 8 March 2007 / Accepted: 29 November 2007 / Published online: 16 December 2007

Abstract The non-transition metal spinel $MgAl_2O_4$ and the transition metal spinels ($NiFe_2O_4$, $NiAlFeO_4$) have been prepared by standard ceramic processing method in the air. The effect of annealing atmosphere on the dielectric properties after sintering has been studied. The annealing atmospheres were N_2, O_2, and N_2–H_2 mixture. Dielectric constant ε_r and tangent loss tanδ have been characterized by varying the measuring temperature and frequency (5 Hz–5 MHz) using the impedance analyzer. The ε_r and tanδ of the non-transition metal spinel $MgAl_2O_4$ remained unchanged even with varying the annealing atmosphere. While the dielectric properties of the transition metal spinels, $NiFe_2O_4$ and $NiAlFeO_4$ were critically dependent on the annealing atmosphere. Crystal structural models for the samples manufactured in air have been tested by the Rietveld refinement method for both the centrosymmetric Fd-3m and the noncentrosymmetric F-43m. The electron density distributions were determined by the whole pattern fitting based on the maximum entropy method (MEM). The dielectric properties of the samples have been also discussed in terms of the structure and electron distribution analysis results.

Keywords Crystal structure · Dielectric property · Annealing atmosphere · Electron density distribution · Spinel oxide

J. S. Kim (✉)
Department of Digital Display, Hoseo University,
San 29-1 Sechul-ri, Baebang-myon,
Asan, Chungnam-do 336-795, South Korea
e-mail: kimjungs@office.hoseo.ac.kr

K. H. Lee · C. I. Cheon
Department of Materials Science and Engineering,
Hoseo University,
Asan, Chungnam 336-795, South Korea

1 Introduction

Spinel oxides show a wide spectrum of electrical properties covering insulating, semiconducting, metallic, and superconducting [1, 2]. The characteristic features of the dielectric and magnetic properties have been known to arise from distribution and type of the cations among the tetrahedral A-site and octahedral B-sites in the structure [3].

The dielectric properties (tanδ, ε_r) dependent on the frequency and measuring temperature have been studied in the previous studies due to many technological applications ranging from microwave to radio frequency of the ferrites, $Li_{0.5}$ $Ni_{0.75-x}Cd_xFe_2O_4$, $Ni_{1-x}Cu_xAlFeO_4$, and $Co_{0.5}Cu_{0.5}$-$Ga_xFe_{2-x}O_4$ [3–6]. In the previous studies the dielectric relaxation phenomena with frequency and temperature have been discussed in terms of the electron and/or hole hopping between the two mixed valence cations $Fe(Ni)^{2+}$–$Fe(Ni)^{3+}$ in the octahedron/tetrahedron [3, 4]. The electron/hole hopping is characteristic of the semiconducting spinels covering the most of the ferrites.

Ponpandian et al. [3] suggested that in spinel ferrites the wave functions of the cation electron are localized and little overlap between the adjacent cations. Hence the electron/hole hopping between the cations should be mediated by the lattice vibration. The ionic distance between the A (tetrahedron)-site is larger (~0.36 nm) than the B(octahedron)-site (~0.29 nm) in transition metal spinels. And the degree of the covalency for the A-site ions is larger than that of B-site cations. Hence the hole mobility due to Ni^{2+}–Ni^{3+} transitions in the A-site is smaller due to a high activation energy than that of the B-sites.

In this study we prepared the non-transition metal spinel $MgAl_2O_4$ and the transition metal spinels ($NiFe_2O_4$ and $NiAlFeO_4$), and characterized the dielectric properties including the dielectric relaxation and tangent loss peak with frequency. The effect of annealing atmosphere (N_2,

O_2, and H_2/N_2) on the dielectric and electrical properties has been compared for these two types of spinels.

The crystal structure of $MgAl_2O_4$ has been generally known as the centrosymmetric Fd-3m. On the while the other noncentrosymmetric model F-43m has been also suggested [7, 8]. In this study we analyzed the crystal structures of the three spinels by Rietveld method and the electron density distributions are determined by the whole pattern fitting based on the maximum entropy method (MEM) [9, 10]. The MPF(MEM-based whole pattern fitting) results are discussed in terms of the dielectric properties. The MEM method has been applied to the visualization of the electron density distribution from the XRD data for decades [10]. In the so-called MEM/Rietveld method developed by Tanaka et al. the 'observed' structure factors, Fo (obtained in the Rietveld) lowers the accuracy of the analyzed three-dimension electron densities, since the 'observed' structure factors, Fo are doubly biased toward the structural model in the Rietveld analysis. The structural refinement by MEM-based whole pattern fitting (MPF) developed by Izumi overcomes these flaws in the procedure of Tanaka et al. Detailed methodology for the MPF method is described some literatures [11–13]. The MPF method has been reported to be effective and adequate for the representation of the average structures for the crystalline materials showing static and dynamic disorder, chemical bonding, nonlocalized electrons. This structural analysis technique has successfully been applied numerous materials systems: zeolite, superconductor, silicate, phosphate, carbon, solid state ionics [14–16].

2 Experimental

Three samples, $MgAl_2O_4$, $NiFe_2O_4$, and $NiAlFeO_4$ have been prepared by the conventional ceramic processing method using the chemical reagents, MgO, Al_2O_3, NiO, and Fe_2O_3 as raw materials. For enhancement of the sinterability of $MgAl_2O_4$ sample, nano-sized Al_2O_3 powder was used as the raw material. The mixture of raw materials was calcined at the temperature range of 1000–1350 °C and then ball milled with 0.5 wt% PVA binder. The dried powder mixture was pressed to disc shape samples and sintered at temperature range of 1250–1600 °C for 5 h in air. The final sintering temperatures for each type of sample were selected to produce the linear sintering shrinkage >15%. The sintered samples were annealed under N_2, O_2, and $10H_2/90N_2$ atmosphere at 1200 °C for 5 h. The $MgAl_2O_4$ showed the linear sinter-shrinkage of 19.78 and 22.25%, respectively, at 1550 and 1600 °C. The ε_r and tanδ have been measured using impedance analyzer over the frequency range 100 Hz–1 MHz. The crystal structure was analyzed by the Rietveld refinement method using the program Reitan2000 using the X-ray diffraction data (Cu-Kα radiation) for the samples sintered in air without post-annealing. The electron density distribution in the samples were determined by the maximum entropy method (MEM)-based whole pattern fitting (MPF) using the MEM analysis software program PRIMA. The 3D electron density distributions are visualized by the software program VEND incorporated in the 3D visualization package, VENUS [11–13].

3 Results and discussion

The effect of annealing atmosphere on the dielectric properties of $MgAl_2O_4$ is shown in Fig. 1. The variation of the annealing atmosphere does not change the dielectric

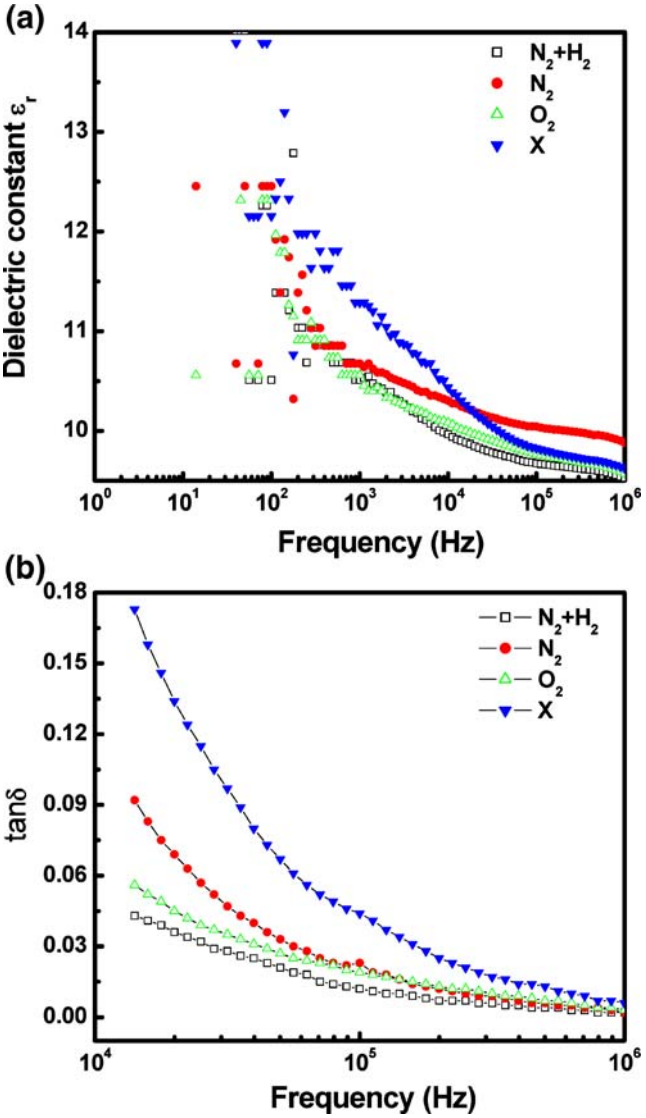

Fig. 1 Effect of annealing atmosphere on the frequency dependent dielectric properties (**a**) ε_r (**b**) tanδ of $MgAl_2O_4$ sintered at 1550 °C in air. (annealed at 1200 °C for 5 h). (The remark *x* implies the as-sintered sample in air)

behaviors. The $MgAl_2O_4$ sample sintered under the N_2/H_2 atmosphere shows the slightly lower values of the ε_r and tanδ compared to other atmosphere conditions. The dielectric constant ε_r (Fig. 1(a)) slightly increases with measuring frequency from 9.5 at 1 MHz to ~12 at 100 Hz. At low frequency the ε_r values show some fluctuations but tend to increase with further lowered frequency. The tanδ values also steadily increase from ~0.006 at 1 MHz to 0.05–0.18 at 1 kHz. The inertness of the $MgAl_2O_4$ to the annealing atmosphere can be rationalized by the fact that the valence values of the Al^{3+} and Mg^{2+} ions does not changed under the annealing atmosphere variation. Table 1 shows the resistivity of the annealed samples under the various atmospheres. The $MgAl_2O_4$ samples show the highest resistivity compared to those of the $NiFe_2O_4$ and $NiAlFe_2O_4$. Among the $MgAl_2O_4$ samples the N_2/H_2 annealing produced the relatively large resitivity in accordance to the dielectric constant. But the effect of annealing atmosphere is not significant in the $MgAl_2O_4$ samples.

The dielectric properties of $NiFe_2O_4$ are shown in Fig. 2. The ε_r increases exponentially with frequency: from 961 (O_2 atmosphere) at 1 MHz to 5.5×10^4 at 100 Hz. The $90N_2/10H_2$ annealed $NiFe_2O_4$ sample cannot be shown in Fig. 2 due to the ε_r exceeds the scale range shown in the Fig. 2. The electrical resistivity of the $NiFe_2O_4$ samples is of semiconducting range as shown in Table 1. The resistivity of N_2 and N_2/H_2 annealed samples cannot be measured even at 1 V due to electrical leakage. The tanδ curve show loss peaks at the range of 1–10 MHz. Generally the tanδ peak appears at the frequency larger than that of the ε_r peak.

Table 1 Effect of annealing atmosphere on the electrical resistivity of the spinel samples at the designated measuring AC voltage.

Sample/atmosphere	Measuring voltage/resistivity	
$MgAl_2O_4$	500 V	100 V
Not annealed (x)	7.25E+13 Ω cm	2.55E+14 Ω cm
O_2	3.48E+13 Ω cm	4.54E+13 Ω cm
N_2	1.23E+14 Ω cm	3.83E+14 Ω cm
N_2+H_2	8.85E+14 Ω cm	4.09E+15 Ω cm
$NiFe_2O_4$	1 V	0.1 V
Not annealed (x)	3.38E+06 Ω cm	Unmeasurable
O_2	3.52E+06 Ω cm	Unmeasurable
N_2	Unmeasurable	2.08E+06 Ω cm
N_2+H_2	Unmeasurable	9.64E+05 Ω cm
$NiAFeO_4$	100 V	50 V
Not annealed (x)	9.98E+07 Ω cm	8.58E+07 Ω cm
Not annealed (x)	500 V	100 V
O_2	Unmeasurable	1.47E+08 Ω cm
O_2	1 V	0.1 V
N_2	1.86E+06 Ω cm	4.74E+09 Ω cm
N_2	1 V	0.1 V
N_2+H_2	Unmeasurable	Unmeasurable

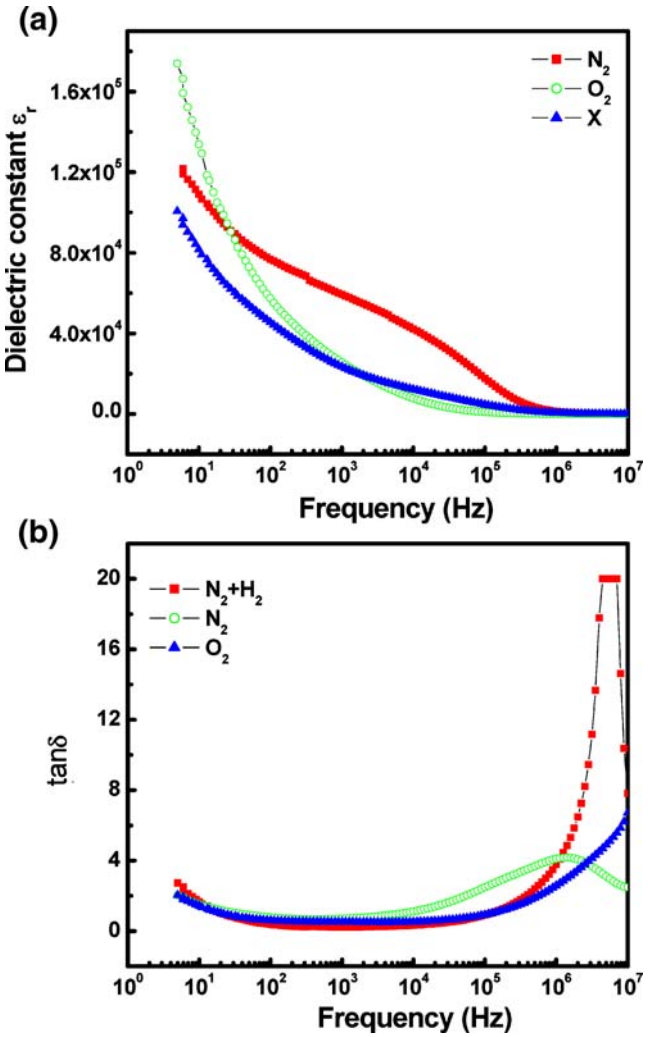

Fig. 2 Effect of annealing atmosphere on the frequency dependent dielectric properties (**a**) ε_r (**b**) tanδ of $NiFe_2O_4$ a sintered at 1600 °C in air. (annealed at 1200 °C for 5 h). (The remark *x* implies the as-sintered sample in air)

The dielectric properties of $NiAlFeO_4$ are shown in Fig. 3. The dielectric constant ε_r (O_2 sample) increases very steadily with frequency compared to that of $NiFe_2O_4$. The ε_r (O_2 sample) increases from 13.9 (at 1 MHz) to 89 at 100 Hz. Then the ε_r increase exponentially at below 1–10 kHz. The tanδ peaks appears at the range of 10 Hz–10 KHz. The oxidizing atmospheres (O_2 and x [air]) produce lower peak frequencies compared N_2 and H_2/N_2.

The tangent loss peaking behavior observed in the $NiAlFeO_4$ and $NiFe_2O_4$ occurs by the resonance of the electron hopping frequency between Fe^{3+} and Fe^{2+} with the applied electric field frequency [4–6]. The hole hopping between Ni^{2+} and Ni^{3+} are considered as to have the lager activation than the electron hopping and becomes appreciable at high temperature. The dispersion in tanδ at lower frequency in the $MgAl_2O_4$ is considered as a different origin such as the silver electrode and specimen correlation.

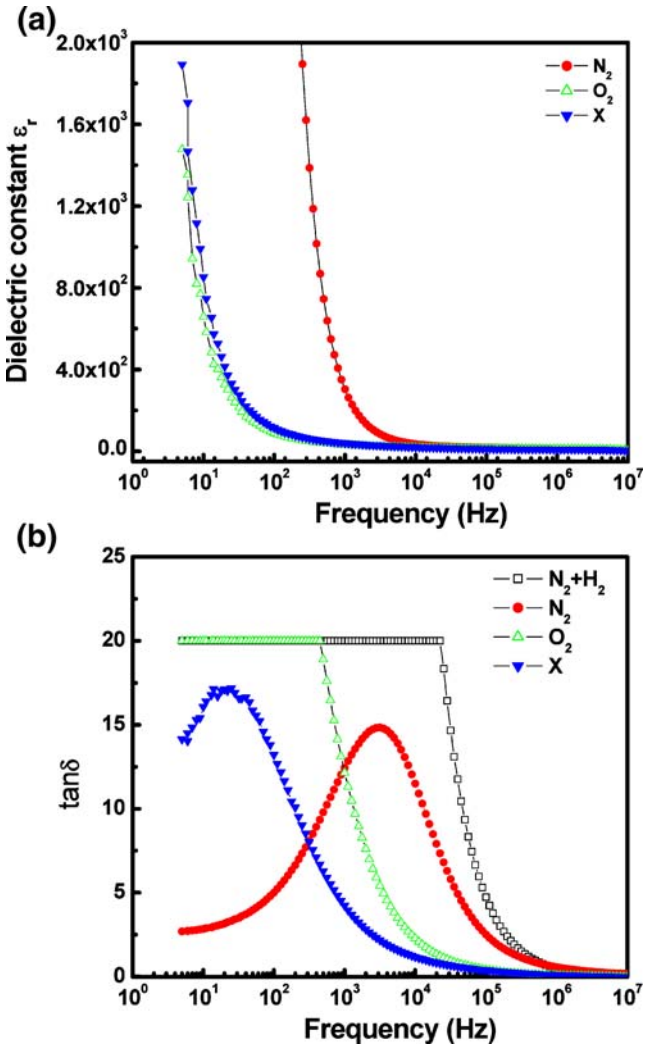

Fig. 3 Effect of annealing atmosphere on the frequency dependent dielectric properties (**a**) ε_r (**b**) tanδ of $NiAlFeO_4$ a sintered at 1350 °C in air. (annealed at 1200 °C for 5 h). (The remark *x* implies the as-sintered sample in air)

The dielectric polarization in the $NiAlFeO_4$ and $NiFe_2O_4$ consists of two components. One is the orientational polarization by the electron hopping between Fe^{2+} and Fe^{3+} [17, 18] which is the dominant mechanism in these two samples. The other minor contribution comes from the ionic and electronic polarizations. In the $MgAl_2O_4$ only the ionic and electronic polarizations operate and hence result in the low ε_r values (~9.5 at 1 MHz, ~12 at 100 Hz) regardless of the annealing atmosphere.

The valence states of Fe^{2+} are the minority while the Fe^{3+} state are the majority in the $NiAlFeO_4$ and $NiFe_2O_4$ But the Fe^{2+} concentration increases by annealing the samples in H_2/N_2 and N_2 atmosphere. Hence the electrical resistivity becomes lower in the H_2/N_2 and N_2 annealed samples than those of the x (not annealed) and O_2 annealed samples. The dielectric constant ε_r increases inversely to that of resistivity. When we consider the electrical and the dielectric constant ε_r of the $NiAlFeO_4$ and $NiFe_2O_4$ in terms of the Fe^{2+} concentration, the Fe^{2+} concentration is doubled in $NiFe_2O_4$ compared to that of $NiFe_2O_4$ simply because of the Fe-ion mole ratio in the chemical formula. In this aspect the electrical resistivity of $NiFe_2O_4$ should be much lower than that of $NiAlFeO_4$ as observed in Table 1.

The $MgAl_2O_4$ has been known as a normal spinel. The $NiFe_2O_4$ is an inverse spinel with 1/2 of the Fe ions occupying the tetrahedron site (Fe^{3+}) and written as the formula $(Fe^{3+})[Ni^{2+}Fe^{3+}]O_4$. The crystal structures of the as-sintered samples without post annealing (marked as x in Figs. 1, 2 and 3) have been analyzed by Rietveld method using the centrosymmetric Fd-3m and the noncentrosymmetric F-43m models. The noncentrosymmetric model always produced lower *R*-values in all the samples. In the $MgAl_2O_4$ the *R*-values were Rwp=11.93, Rp=8.55, *S*=1.40,

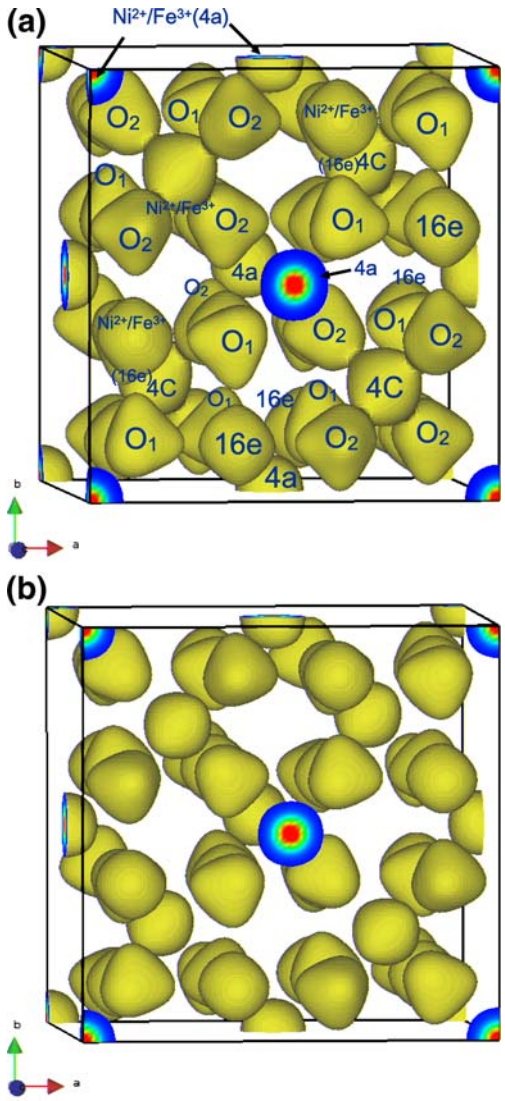

Fig. 4 Electron density distribution determined by MPF(MEM-based pattern fitting) method for the (**a**) $NiAlFeO_4$ (**b**) $MgAl_2O_4$. Isosurfaces in the unit cells are drawn for the eui-electron density level of 1.0/Å^3

RI=:4.70, RF=3.54% (Rwp=21.3, Rp=14.0, Re=8.49, S=2.51, RI=13.7, RF=8.25%). In the parenthesis the R-values produced by the centrosymmetric Fd-3m model are shown.

In the $NiFe_2O_4$ sample ($a=b=c$=8.329 Å,) the Rietveld analysis showed the R-values of Rwp=6., Rp=5.1, Re=5.6, S=1.14, RI=2.14, RF=2.32%. And the cation site occupancies are Ni^{2+}/Fe^{3+}=0.26/0.74 (4a and 4c-site: multiplicity and Wyckoff letter, tetrahedral) and Ni^{2+}/Fe^{3+}=0.63/0.37 (16e-site: octahedral). Three quarters of the Ni^{2+} ions occupy the octahedral site (inverse spinel), but about 26% ions are mixed into the tetrahedral site (normal spinel).

In the $NiAlFeO_4$ sample (a=8.1858 Å) the Al^{3+} ions are fairly equally distributed both in the tetrahedron and octahedron sites (26–36% occupancy). The electron density distribution determined by MPF (MEM-based pattern fitting) method is shown in the Fig. 4 for the $NiAlFeO_4$ and $MgAl_2O_4$ samples. The R-values after the MPF analysis were Rwp=7.15, Rp=5.70, S=1.17, RI=4.97, RF=5.07%.

The electron density distribution in the unit cell can represent the characteristic features of the chemical bonding, e.g., covalent/ionic and the nature of electrons, e.g., localized/nonlocalized. Hence the determined average electron density distribution by MPF method can be discussed with fair means in relation with the dielectric properties of the spinel samples. In Fig. 4(a) the electron density distribution for the $NiAlFeO_4$ shows that the tetrahedral 4c-site ($x=y=z$=0.25, 4c: multiplicity and Wyckoff letter) cations have relatively strong covalent bonds with coordination oxygens. However the other tetrahedral cations (4a-site) show nearly isotropic electron density distribution which implies relatively more ionic bonds. The electron density distribution around the oxygen sites (O1 and O2) show very anisotropic features. Since the 4c-site (A-site) is strongly covalent, the Ni^{2+}–Ni^{3+} hole transition is expected to be smaller than in the B-sites [4–6] based on the discussion in the introduction concerning the dielectric properties of $NiFeO_4$. The electron density distribution in the $MgAl_2O_4$ is shown in Fig. 4(a) for the comparison to that of $NiAlFeO_4$. The iso-surfaces of electron densities (1.0/Å^3) show that the electrons are distributed over the reduced volume around the ion centers in the $MgAl_2O_4$. Hence the electron/hole hopping chances between the cations, i.e. the cation–oxygen–cation exchange would scarcely happen.

4 Conclusion

The dielectric properties of the non transition ionic $MgAl_2O_4$ does not change with the annealing atmosphere while those of the transition ionics, $NiFe_2O_4$ and $NiAlFeO_4$ are exponentially dependent on the annealing atmosphere. The electron hopping between Fe^{3+} and Fe^{2+} leads to the large dielectric constant and dielectric relaxation in these samples. The non transition ionic $MgAl_2O_4$ does not show a dielectric relaxation except in the very low frequency <200 Hz. In the $MgAl_2O_4$ only the electronic and ionic polarizations contribute to the dielectric constant and result in the low ε_r (~10).

The crystal structures of three samples were decided as the noncentrosymmetric F-43m. In the $NiAlFeO_4$ the Al^{3+} ions are fairly equally distributed both in the tetrahedron and octahedron sites (26–36%). The high degree of the covalence at one of the A-site can be confirmed by the MEM-based pattern fitting method. In the $NiAlFeO_4$ the electron density distribution shows that the tetrahedral 4c-site cations ($x=y=z$=0.25) have relatively strong covalent bonds with the coordinated oxygens. The other tetrahedral 4c-site show isotropic electron density distribution. The equi (iso)-electron density surfaces are distributed over the reduced volume around the ion centers in the $MgAl_2O_4$ leading to the electron/hole hopping between the cation–oxygen–cation exchange would be much scarcely occurs.

Acknowledgments This work was supported by Grant No. R01-2007000-11000-0 from the Basic Research Program of Korea Science and Engineering Foundation.

References

1. C. Gleitzer, J.B. Goodenough, *Mixed valence Iron Oxides, Structure and Bondings*, vol. *61* (Springer, Berlin, 1985), pp. 1–70
2. A. Angappan, L.J. Berchmans, C.O. Augustin, Mater. Lett **58**, 2283 (2004)
3. N. Ponpandian, P. Balaya, A. Narayanasamy, J. Phys: Condens. Matter **14**, 3221 (2002)
4. R.G. Kharabe, R.S. Devan, C.M. Kanamadi, B.K. Chougule, Smart Mater. Struct. **15**, N36–N39 (2006)
5. M. Kaiser, Phys. Stat. Sol. **201**(14), 3148 (2004)
6. S.S. Ata-Allah, K.K. Fayek, Phys. Stat. Sol. **175**, 725 (1999)
7. N.W. Grimes, J. Phys.: Condens. Matter **4**, L567–L570 (1992)
8. S. Collyer, N.W. Grimes, D.J. Vaughan, J. Phys. C: Solid State Phys. **21**, L989 (1988)
9. F. Izumi, Mat. Sci. Forum **59**, 378–381 (2001)
10. M. Takata, E. Nishobori, M. Sakata, Z. Kristallogr. **71**, P216 (2001)
11. F. Izumi, Olid State Ionics **172**, 1–6 (2004)
12. A.A. Belik, F. Izumi, T. Ikeda, V.A. Morozov, R.A. Dilanian, S. Torii, E.M. Kopin, O.I. Lebedev, G. Van Tendeloo, B.I. Lazoryak, Chem. Mater. **14**, 4464 (2002)
13. N. Kijima, T. Ikeda, K. Oikawa, F. Izumi, Y. Yoshimura, Solid State Chem. **177**, 1258 (2004)
14. K. Takada, H. Sakurai, E. Takayama-Muromachi, F. Izumi, R.A. Dianian, T. Sasaki, Nature **422**, 53 (2003)
15. M. Takada, E. Nishibori, M. Shinmura, H. Tanaka, K. Tanigaki, M. Kosaka, M. Sakata, Mater. Sci. Eng. **A312**, 66 (2001)
16. T. Noritake, S. Towata, M. Aoki, Y. Seno, Y. Hirose, E. Nishibori, M. Takata, M. Sakata, J. Alloys Compd. **356**, 84 (2003)
17. S.A. Olofa, J. Magn. Magn. Mater. **131**, 103–106 (1994)
18. M.A. Ahmed, E. Ateia, I.M. Salah, A.A. El-Gamal, Phys. Status Solidi **201**(13), 3010 (2004)